

Estimating the Seismic Strength of Infill Walls by Means of Hollow Brick Prism Tests

Eray Özbek^{1*}, Osman Karakuş¹

¹ Department of Civil Engineering, Faculty of Engineering, Gazi University, Ankara, 06570, Turkey

* Corresponding author, e-mail: erayzbek@gazi.edu.tr

Received: 19 June 2022, Accepted: 09 October 2022, Published online: 19 October 2022

Abstract

Architectural infill walls interact with the surrounding reinforced concrete load bearing members of the building under lateral earthquake loads and can change the system behavior significantly. Therefore, lateral strength calculation of these walls may become mandatory for the designers. These infill walls often formed with horizontally-hollow clay based bricks in many regions of the world. However, strength of these bricks depends on the loading direction and bricks remain in the diagonal compression strut of an infill wall are subjected to biaxial compression. Thus, testing procedures investigate the strength only in the direction perpendicular to the bed-joint seems insufficient to reflect actual behavior. Accordingly, it is confusing for designers to determine or consider compressive strength of hollow clay bricks in order to model and calculate the strength of an infill wall. To clear up this confusion, the seismic strength of plastered infill walls made up of horizontally-hollow bricks were tried to be estimated by various prism tests. The effects of loading direction, plaster, and presence of a single or double brick on prism strength were experimentally investigated. Six reference walls and more than 170 prism specimens were tested in accordance with this scope. The correlation between prism and infill wall strength was established with a valid and practical method. Results showed that diagonally loaded plastered prism group successfully and adequately estimated the experimental infill wall strength. In addition, if diagonal testing is not possible to conduct, the average strength of the vertically and horizontally loaded prism tests may be used instead.

Keywords

brick, strength, brick wall, loading direction, ASTM C1314

1 Introduction

Due to its low cost, heat resistance and relatively light weight, the infill walls of reinforced concrete (RC) structures are often formed with horizontally-hollow bricks. Although these infill walls are not generally included in the calculations as a load bearing member, they can significantly change the system behavior of the building by interacting with the RC members of the building under lateral earthquake loads. This behavior change is perceived by many engineers as a positive contribution to structural stiffness and strength [1]. Therefore, it is claimed that neglecting the infill wall behavior is a safe approach. However, recent research has indicated that such an approach can result misleading and dangerous consequences. Under the earthquake loads, infill walls can lead to shear failure of RC members even designed in accordance with the principles of ductility [2–8]. Thus, it is especially required to ensure that surrounding RC columns and beam-column joints have sufficient shear resistance against the ultimate load

that can be transmitted from the infill wall. In this study, infill walls refer to solid infill walls surrounded by an RC frame. Readers can review other studies on the behavior of infill walls with openings for windows or doors [9–11]. There are several modes of infill wall failure such as bed-joint sliding, diagonal cracking, and corner crushing. Among these, corner crushing is the strongest and stiffest one [12]. Therefore, infill wall strength, especially this type of compression strength and behavior should be estimated with satisfactory accuracy. Even though there are sophisticated and accurate methods to model infill walls, equivalent diagonal strut model is the most practical one [13, 14]. FEMA-306 from 1998 states that lateral strength of the infill wall according to corner compression failure (V_c), can be calculated by using the Eq. (1) while modelling the infill wall as an equivalent diagonal strut [12].

$$V_c = a_{inf} t_{inf} f_{me90} \cos \theta \quad (1)$$

Where a_{inf} is the equivalent width of compression strut; t_{inf} the thickness of infill panel; f'_{me90} the expected strength of masonry in the horizontal direction; θ the angle whose tangent is the infill height-to length aspect ratio, radians. As seen, accuracy of the Eq. (1) depends on the reliability of the f'_{me90} value. Instead of determining this strength, FEMA-306 [12] permits to take 50% of the expected (mean value of the population) stacked prism compressive strength (f'_{me}). However, a_{inf} in this equation needs vigorous calculations.

On the other hand, ASCE/SEI 41-17 [15] adopts Eq. (2) which practically assumes bearing length of the compression strut is one-third of its height.

$$F_{mc} = f'_m (h_{inf} / 3) t_{inf} \quad (2)$$

Where F_{mc} is the bearing (compressive) strength of the infill and h_{inf} is the height of the infill wall. f'_m is the lower-bound (specified) masonry compressive strength which means f'_{me} minus one sample standard deviation (STD) of the strengths. On the other hand, f'_{me} can also be taken as $1.3 f'_m$ [12]. It can be noted that, F_{mc} is the strength in the diagonal direction, so should be multiplied by $\cos\theta$ to obtain lateral strength as in Eq. (1).

ASCE/SEI 41-17 [15] refers TMS 602-13 [16] to determine f'_{me} based on masonry prism tests. The prism test method is described in ASTM C1314-14 [17]. Accordingly, masonry prism specimens are constructed by using the same materials in the actual construction such as bricks, mortar, and grout or obtained from field-removed specimens. Regardless of the alignment in the actual wall, prisms are built in stack bond style with a full mortar bed joint. Prisms should have a minimum of two bricks with height-to-thickness ratio between 1.3 and 5.0. Prisms are tested in the compression machine and strength is calculated from the ultimate load divided by the prism cross-sectional area. Effect of the aspect ratio is also taken into account with some correction factors.

As a matter of course, ASTM C1314-14 [17] is based on the common brick types used in the United States. In the United States, infill walls are usually composed of solid clay or concrete units. Although hollow clay tile (brick) was widely utilized until the 1950s, it has nearly vanished from the construction since then [18]. On the other hand, infill wall brick types, features and usage are varied from one region to another in the world. As opposed to United States, hollow clay bricks are still popular in the Southern Europe [19–21], Middle East [22, 23], and South

America [24]. Moreover, those walls are coated with a concrete plaster and ASTM C1314-14 [17] also does not cover plastered brick units. Research indicate that plaster on the infill wall surface can make a significant contribution to strength [25]. On the other hand, these hollow bricks are placed in a way that their holes are in horizontal direction during the bricklaying and strength of those bricks depend on the direction of loading [22]. It should be noted that even solid clay bricks show clear anisotropic behavior [26]. Thus, testing procedure in ASTM C1314-14 [17] investigate the strength only in the direction perpendicular to the bed-joint seems insufficient. Additionally, bricks remain in the diagonal compression strut of an infill wall are subjected to biaxial compression rather than the uniaxial one. Accordingly, it is confusing for designers to assume, test or take into account compressive strength of hollow clay bricks in order to model and calculate the strength of an infill wall diagonal compression strut. It is intended to provide data that can guide engineers in their design process.

Therefore, experimental research was conducted in order to obtain infill wall lateral strength by means of various prism testing methods including ASTM C1314-14 [17]. The results and their ability to represent actual infill wall behavior was discussed. The methods are also compared among themselves and the correlation between them were tried to be revealed analytically. New methods and practical rule of thumbs were suggested to estimate the strengths with acceptable accuracy. In order to make a more accurate evaluation, the number of specimens was kept as much as possible. Six reference walls and more than 170 prism specimens were tested in accordance with this scope.

2 Experimental study

2.1 Test specimens

Six infill wall panels were constructed and tested under reversed cyclic lateral loading. These six infill walls were reference specimens and identical to each other. Since infill walls are not usually included in the calculations as a primary load bearing member, they are not built with the concern of standard strength. Thus, the standard deviation of hollow bricks in terms of strength are rather high compared to structural concrete. Therefore, the total number of reference specimens was chosen as six in order to make more accurate and statistical evaluation. The geometry and details of the prepared reference specimens are shown in Fig. 1. These identical reference specimens were named as R1 to R6 for convenient evaluation of the test results.

Considering the laboratory conditions, reference plastered infill walls having dimensions of 1490 mm width and 1172 mm height were built. The wall thickness was 100 mm with an 8 mm plaster thickness applied to both faces (Fig. 1(a)).

The infill walls were constructed with 85 × 190 × 190 mm hollow clay bricks. Note that these are nominal dimensions and measured dimensions are 84 × 187 × 187 mm (Fig. 1(b)).

Bricks were placed in a way that their holes are in horizontal direction during the bricklaying in accordance with the general practice and the Turkish Standard TS EN 771-1 [27]. Mortar joint thickness was 10 mm in both horizontal and vertical directions. Finally, the wall faces were covered with thin gypsum plaster. That was in order to observe the cracks better during the experiment and to increase the clarity of the pictures taken. This process is also done in most of the actual local practices to prepare smooth wall surfaces for painting.

Prism specimens were constructed simultaneously with the infill walls by using same materials. Test group names were selected to represent test parameters (Fig. 2). The letter "S" was for "Specimen". Following letter "V", "H", or "D" indicated the direction of loading as "vertical", "horizontal", or "diagonal", respectively. Note that while "vertical" corresponded to loading in the direction of hollows in the brick, "horizontal" corresponded to loading in the transverse direction of hollows as shown in Fig 2. Next letter "B" or "P" denoted if the test prisms were "Bare" or covered with a "Plaster" by their initials. The number at the end (1 or 2) represented the number of bricks in a stack.

Properties and number of prism specimens in each group is summarized in Table 1. A total of 178 prism specimens were tested. Among these, the group SVB-2 was based on ASTM C1314-14 [17] which had double bricks in a stack with mortar and no plaster. The loading was in the

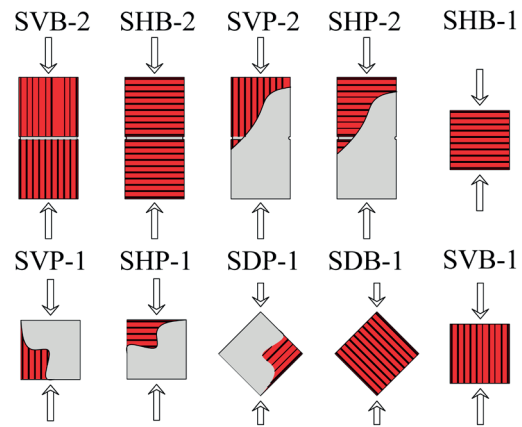


Fig. 2 Prism specimens and their direction of loading

Table 1 Prism test specimens

specimen group	loading direction	plaster	bricks in a stack	number of tests
SVB-2	vertical	no	double	10
SHB-2	horizontal	no	double	10
SVP-2	vertical	yes	double	10
SHP-2	horizontal	yes	double	10
SVP-1	vertical	yes	single	21
SHP-1	horizontal	yes	single	21
SDP-1	diagonal	yes	single	21
SVB-1	vertical	no	single	30
SHB-1	horizontal	no	single	30
SDB-1	diagonal	no	single	15

direction of hollows. In other words, this is the corresponding test procedure, if the designer adopts ASTM C1314-14 [17] to perform prism tests on horizontal hollow clay bricks. The SVB-2 group had mortared joint thickness of 10 mm as reference walls.

Contrary to USA practice, since hollow bricks are placed horizontally during bricklaying, the SHB-2 group was formed. Accordingly, bricks in the stack were placed

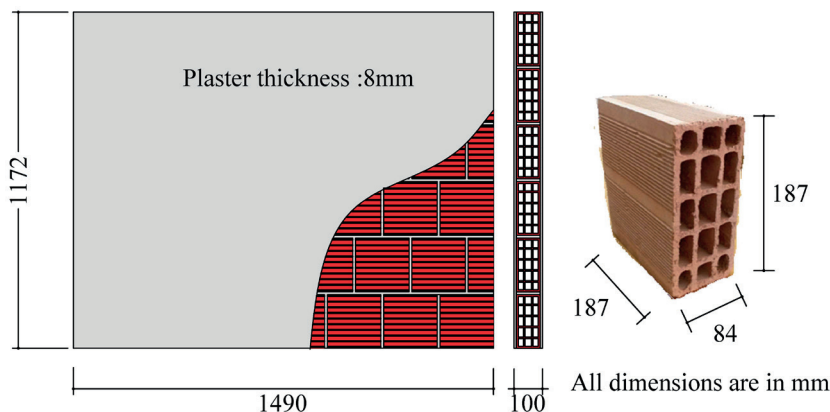


Fig. 1 Reference specimens (a) and hollow bricks (b)

horizontally, unlike the group SVB-2. On the other hand, because plaster may also contribute significantly to the prism strength, group SHP-2 and SVP-2, which are plastered versions of group SHB-2 and SVB-2, were tested. These groups had plaster thickness of 8 mm on both faces as in reference walls (Fig. 2). Each double brick prism group had identical 10 specimens.

The method in ASTM-C1314-14 [17] is labor-intensive and time-consuming since it requires building prisms with minimum two bricks with mortar beds. Moreover, heights of prism specimens are generally too large for compression machines which are originally produced for concrete cylinder specimens. Thus, single brick versions of the prisms SVB-2, SHB-2, SVP-2, and SHP-2 were constructed as SVB-1, SHB-1, SVP-1, and SHP-1 in order to research their correlation among each other (Fig. 2). SVB-1 and SHB-1 group were also used to evaluate strength properties of hollow clay bricks. While plastered groups composed of 21 specimens, bare groups composed of 30 specimens (Table 1).

Bricks especially in the corner regions of the diagonal compression strut are subjected to biaxial compression due to rotational movement of columns and closing up of beams in an RC frame. To reflect this analogy, single brick prisms of SDP-1 and SDB-1 were tested in the diagonal direction (Fig. 2). Group SDP-1 had plaster thickness of 8 mm on both faces, unlike the group SDB-1. This type of prism testing can be considered new and experimental setup specific to diagonal testing of prism was also developed. SDP-1 and SDB-1 group had identical 21 and 15 specimens, respectively (Table 1).

2.2 Materials

Hollow bricks were part of the same shipment material of the same factory. These bricks, made of clay, are specifically manufactured for masonry infill walls according to TS EN 771-1 [27] and commercially available under the name of horizontally-hollow bricks with nominal dimensions of $85 \times 190 \times 190$ mm. On the other hand, measured dimensions were $84 \times 187 \times 187$ mm. One brick weighed about 20 N and the net area of the surface with hollows was calculated as 6500 mm^2 . In other words, ratio of the gross area to the net area was about 2.5. The surface pattern of the bricks used in the study is shown in Fig. 1(b).

SVB-1 and SHB-1 group were also used to obtain strength properties of hollow bricks. According to the compression test results of 30 specimens in each group (Table 1), while the mean strength, f_{me} , in the direction

of hollows (SVB-1) was computed as 4.00 MPa with an STD of 0.95 MPa, 1.17 MPa with an STD of 0.47 MPa was computed in the transverse direction of hollows (SHB-1). In addition, coefficient of variation (COV) was respectively found as 23.68% and 40.59% for SVB-1 and SHB-1. Note that gross area was considered for the strength calculations.

The mixing ratios of the mortar in terms of volume was 6:1:2:1.5 for sand, lime, cement, and water, respectively. Sieved sand was in the range of 0–3 mm. This mortar was used in both joints and plastering (Fig. 1(a)).

Cube specimens with the dimensions of $100 \times 100 \times 100$ mm were taken from the mixture at the time of construction to determine compressive strength. Cube specimens were tested simultaneously with the brick walls. A total of 24 cube specimens belonged to the plaster and 16 cubes belonged to the joints. Since the mixing ratio of the mortar was same for both joints and plaster, they were assessed together. Accordingly, the mean compressive strength of the mortar (f'_{cm}) was computed as 13.0 MPa with an STD of 1.3 MPa and a COV of 10%. 100×100 mm cubic strength values may be multiplied by 0.8 to convert to the standard 150×300 cylinder strength [28]. It can be noted that ASTM C109 [29] uses 50×50 mm cubes to determine strength of hydraulic cement mortars.

2.3 Test setup and instrumentation

Infill wall specimens, R1 to R6, were placed inside the steel frame which had pins (hinge) at four corners and tested under reversal cyclic lateral loading (Fig. 3). Thus, infill walls interacted with the surrounding frame similar to actual conditions. In other words, boundary conditions, contact surfaces between the wall and frame, were determined by the specimen behavior. Moreover, strength contribution of the surrounding frame was eliminated via the pins. Lateral loading was provided by a double-acting hydraulic jack with a rate that can be considered quasi-static. While one end of the jack was attached to a rigid wall, the other end was attached to the load cell and the load was transferred through the hinges (Fig. 3).

Lateral displacement was measured with the LVDT-1 (linear variable differential transducer) placed in the central axis of the beam on the steel frame. The relative horizontal movement of the steel frame foundation to the rigid floor was measured with the LVDT-2. Displacement of LVDT-2 was very close to zero during each experiment carried out. Diagonal measurements were taken from the specimen with LVDT-3 and LVDT-4 to obtain shear deformations (Fig. 3).

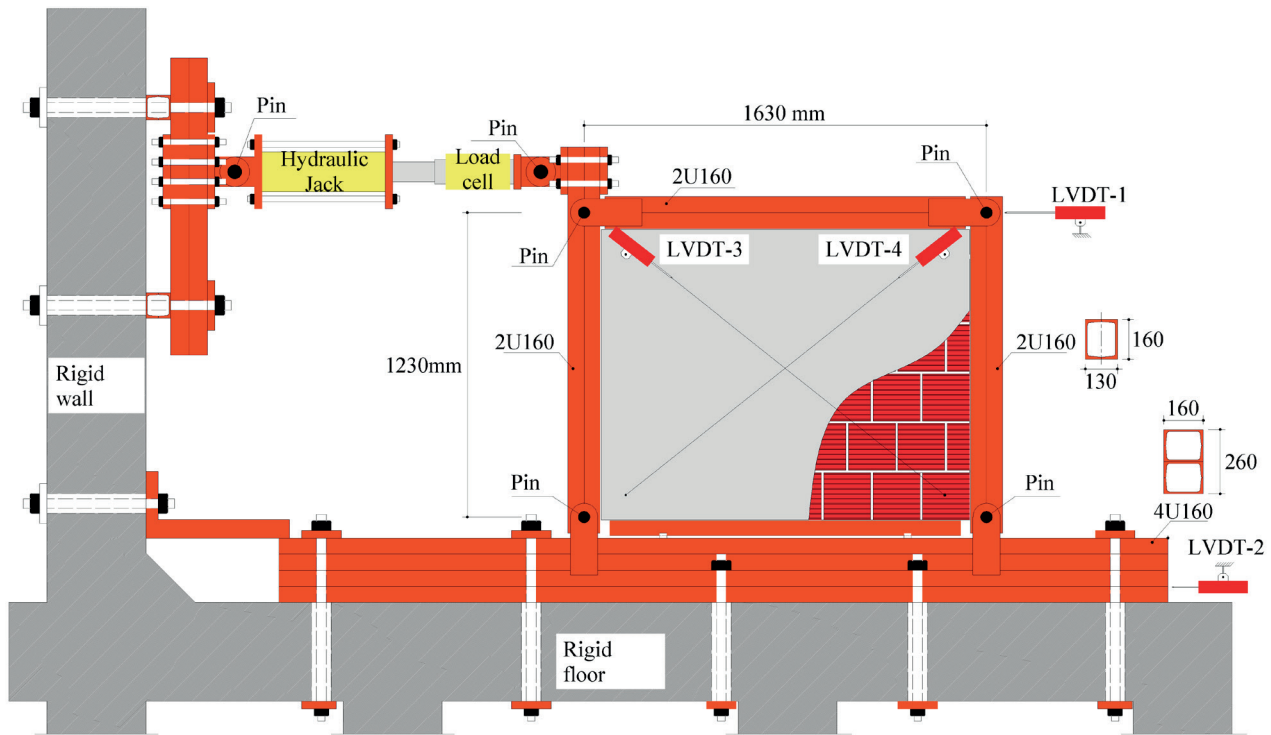


Fig. 3 Test setup for reference infill walls

Same loading program was applied to all infill wall test specimens. Initially, specimens were loaded to 10 kN in the forward (push), then in the backward (pull) direction to complete the first cycle. After that the load was increased by 10 kN in each cycle until any major difference in stiffness was observed. When a major drop in stiffness was observed, displacement controlled loading was applied to be able to force the wall similarly in both directions.

Tests were continued until at least 20% loss of ultimate strength and terminated when the displacement capacity of the test setup (± 125 mm) is reached.

The prism specimens were tested in the compression machine (typically made for concrete specimens) shown in the Fig. 4. Loading rate was held constant for each test at 1.0 MPa/s. This rate was selected also to provide the value for compression test of hardened concrete specimens according to TS EN 12390-3 [30].

A new steel apparatus was built to test prisms diagonally in the compression machine (Fig. 4(b)). Details are shown in Fig. 5. As in the cylinder concrete specimens, a cap was not formed. Instead, cardboard paper was placed to prevent local damages due to the roughness of loading faces of the specimens (Fig. 4). Self-weight of the apparatus on the top was considered negligible when compared to the loads achieved in the tests.



Fig. 4 Orthogonal (a) and diagonal (b) loading of prisms

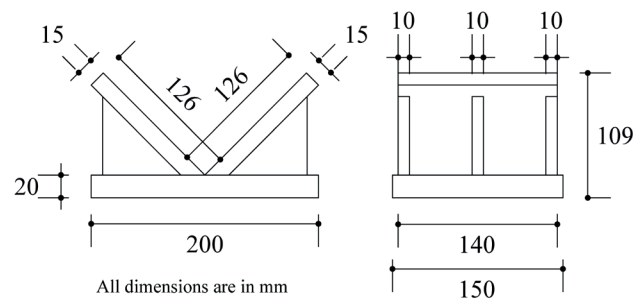


Fig. 5 Geometry of the apparatus used to test prisms diagonally

2.4 Evaluation of experimental results

Applied lateral load versus lateral displacement measured by LVDT-1 (Fig. 3) was plotted for reference infill walls (R1 to R6) and shown in Fig. 6. Related failure modes are also shown in Fig. 7.

The ultimate lateral load in the directions of push and pull is summarized for each specimen in Table 2. The average strength values shown in the Table 2 are the arithmetic mean of the two maximum values obtained from each direction. Since it is not within the scope of the study, criteria such as ductility, stiffness, and energy dissipation were not evaluated.

All of the infill walls experienced corner crushing failure (Fig. 7). Apparent diagonal cracks were not observed. In other words, sudden loss of load (at least 20%) occurred due to the crushing of the bricks on the corner regions. The strength differences between the push and pull directions were quite small. Although this difference was at most 15 kN, it decreased to 1.3 kN when calculated by taking the arithmetic average of the strengths in the push and pull direction (Table 2). On the other hand, the failure loads of the infill walls varied between 77 kN and 111 kN.



Fig. 7 Failure modes of the reference infill walls

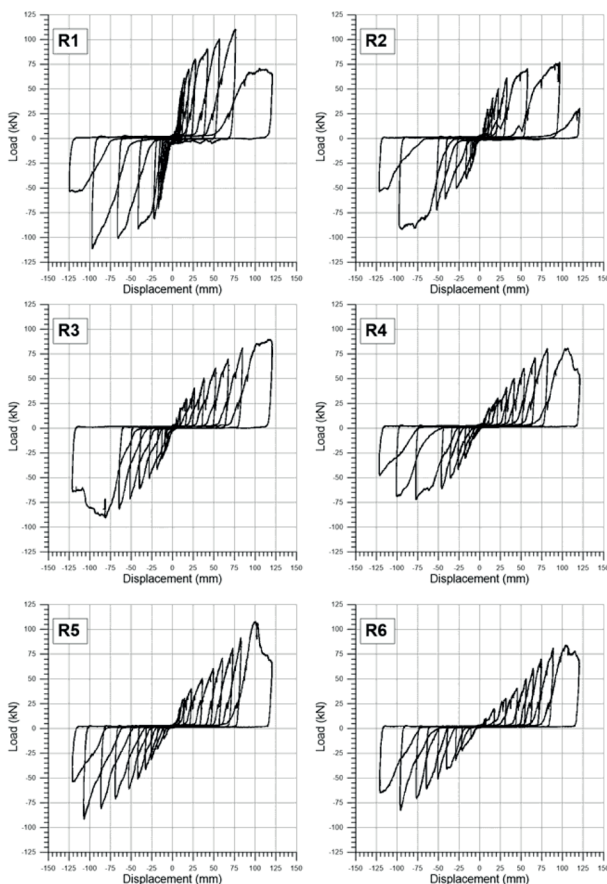


Fig. 6 Load-displacement curves of the reference infill walls

Table 2 Experimental results of infill wall specimens

Infill wall specimen	Ultimate load (kN)			Failure mode	
	push	pull	\bar{x}	push	pull
R1	110	111	111	CC	CC
R2	77	92	85	CC	CC
R3	89	91	90	CC	CC
R4	81	72	77	CC	CC
R5	108	92	100	CC	CC
R6	84	83	84	CC	CC
Average	91.5	90.2	90.8		

\bar{x} : arithmetic mean of push and pull values, CC: Corner Crushing

The average strength of the infill walls was computed as 90.8 kN with an STD of 12.4 kN and a COV of 13.6%.

Results of the prism compression tests are summarized in Table 3. Mean ultimate loads are the arithmetic average of the peak loads measured during the tests. These values were divided by gross cross-sectional area of the prisms (brick+ plaster, if any) to obtain strength values (f'_p) for orthogonally loaded prisms. On the other hand, diagonal gross cross-sectional area of the prisms (brick+ plaster, if any) was considered for diagonally loaded prisms. Height-to-thickness ratio (h_p/t_p) affects the compressive strength of the masonry prisms. Thus, calculated f'_p values multiplied by the correction factor (γ) obtained from ASTM C1314-14 [17]. Here, h_p/t_p was computed using the

height and the least lateral dimension (84 mm) of that prism. The correction factor was determined by linear interpolation between the corresponding h_p/t_p values in Table 1 of ASTM C1314-14 [17].

The correction factors gave consistent results to obtain standard strength. Prisms composed of double bricks according to ASTM C1314-14 [17] had corrected strengths slightly less than the prisms composed of single brick. Among those, the deviation was at most 0.14 MPa for the group SVP-2 and its corresponding group SVP-1. Average deviation was as small as 0.03 MPa which can be considered negligible (Table 3). As a result, the prisms composed of single brick sufficiently represented the double brick specimens if correction factors in ASTM C1314-14 [17] were adopted.

The presence of plaster increased the load bearing capacity of the prisms. On the other hand, the increase in prism strength remained limited as the cross-sections increased with plastering. However, load capacity of the brick plus load capacity of the plaster did not give the realistic results for the load capacity of the plastered bricks. Instead of this direct approach, including half of the plaster strength into calculations gave much more accurate results. In other words, if $0.8 f'_{cm}$ was multiplied by 0.5 and cross sectional-area of the plastered section, plaster capacity for orthogonal and diagonal section was found as 15.6 kN and 22.0 kN, respectively. Note that coefficient of 0.8 was to convert cubic strength values to the standard 150×300 cylinder strength [28]. Experimental load capacity difference between SVP-2 and SVB-2 is 15.4 kN, SHP-2 and SHB-2 is 15.4 kN, SVP-1 and SVB-1 is 12.1 kN, SHP-1 and SHB-1 is 17.3 kN, SDP-1 and SDP-2 is 22.2 kN (Table 3). Thus, maximum deviation from the experimental load capacity was calculated as 5% and calculated capacities were almost equal to experimental load capacities in average. It was

concluded that the reason for the contribution of the plaster which is on the outer surface to remain at 50% level is the lack of confinement.

Vertically loaded specimens had significantly greater strength than the horizontally loaded specimens. Vertically loaded bare prisms 3.6 times and vertically loaded plastered prisms 2.2 times greater strength than the corresponding horizontally loaded prisms in average (Table 3). Arithmetic average in terms of strength values of vertically (SVB-1 & SVP-1) and horizontally (SHB-1 & SHP-1) loaded specimens gave almost equal results, 2.51 kN and 2.96 kN, to the experimental values of diagonally loaded (SDB-1 & SDP-1) specimens as 2.61 kN and 3.06 kN, respectively (Table 3).

COV values of prisms varied between 7.84% and 40.84%. Plastered prisms had less COV values than the corresponding bare prisms except the group SVP-1. Additionally, average of the COV values of the plastered and bare specimens were calculated as 19.8% and 25.0%, respectively (Table 3). As could be seen, COV values of plastered prisms much closer to the COV values of the reference infill walls.

3 Analytical study

As mentioned in previous sections, the average strength of the infill walls was computed as 90.8 kN with an STD of 12.4 kN and a COV of 13.6%. Expected Strength was defined as the mean strength and lower-bound strength was defined as the mean minus one STD of the yield strengths in ASCE/SEI 41-17 [15]. Upper-bound was taken as the mean plus one STD of the yield strengths with the same approach. Thus, expected lateral strength of the reference infill wall (V_{infe}) was 90.8 kN, lower-bound strength (V_{infl}) was 78.4 kN, and upper-bound strength (V_{infu}) was 103.2 kN according to the test results.

Table 3 Experimental results of prism specimens

Specimen group	Mean ultimate load (kN)	Cross-sectional area (mm ²)	Correction Factor (γ)	f'_p (MPa)	$f'_{me} = \gamma f'_p$ (MPa)	STD (MPa)	COV (%)
SVB-2	52.06	15708	1.19	3.31	3.94	0.36	10.89
SHB-2	14.15	15708	1.19	0.90	1.07	0.18	19.47
SVP-2	67.48	18700	1.19	3.61	4.30	0.28	7.84
SHP-2	29.53	18700	1.19	1.58	1.88	0.27	17.27
SVP-1	74.88	18700	1.01	4.02	4.16	1.21	29.97
SHP-1	35.62	18700	1.01	1.90	1.92	0.54	28.36
SDP-1	77.50	26440	1.01	2.93	2.96	0.46	15.71
SVB-1	62.76	15708	1.01	4.00	4.04	0.95	23.68
SHB-1	18.36	15708	1.01	1.17	1.18	0.47	40.59
SDB-1	55.31	22214	1.01	2.49	2.51	0.76	30.50

Eq. (2) in ASCE/SEI 41-17 [15] was adopted for the calculation of infill wall strengths and rewritten as Eq. (3).

$$V_{infe} = f'_{me} \left(h_{inf} / 3 \right) t_{inf} \cos \theta \quad (3)$$

Where h_{inf} is the height of the infill wall, t_{inf} is the thickness of infill panel, θ is the angle whose tangent is the infill height-to length aspect ratio, radians, f'_{me} is the expected (mean value of the population) stacked prism compressive strength. Note that if V_{infl} and V_{infu} are investigated, $f'_{me} - \text{STD}$ and $f'_{me} + \text{STD}$ shall be substituted for f'_{me} in the Eq. (3). Analytical strengths of infill walls which were computed due to Eq. (3) and their comparison to experimental results are shown in Table 4.

Vertically loaded prism group constantly over-estimated the experimental infill wall strength for expected, upper-bound, and lower-bound strengths. The difference was 1.4 times in average and reached up to 1.6 times.

On the other hand, horizontally loaded prism group constantly under-estimated the experimental infill wall strength for expected, upper-bound, and lower-bound strengths. The difference was 0.5 times in average and decreased to 0.3 times. Unlike these results, diagonally loaded plastered prism group, SDP-1, successfully and sufficiently estimated the experimental infill wall strength for expected, upper-bound, and lower bound strengths (Table 4). Since COV values of the SDP-1 group was higher than the infill walls (Table 3), upper-bound and lower bound strengths were slightly deviated as 1.02 and 0.98 times, respectively. However, these differences were resulted in the safe side of the approach and can be considered negligible (Table 4).

It should be kept in mind that arithmetic strength averages of vertically and horizontally loaded prisms (93.3 kN and 80.1 kN) gave almost equal results to the diagonally loaded prisms (90.9 kN and 77.1 kN). Thus, similar suffi-

cient accuracy can be observed by taking into account arithmetic averages of vertically and horizontally loaded plastered prisms (Table 4).

Presence of a plaster on the prism had considerable impact on determining infill wall strength. Calculations even based on diagonally loaded bare prisms had 20% less infill wall expected strength compared to experimental results (Table 4).

4 Conclusions

In this study, the seismic strength of plastered infill walls consisting of horizontal hollow clay bricks were tried to be estimated by prism tests. The effects of loading direction, plaster, and presence of a single or double brick on prism strength were experimentally investigated. Prisms which were prepared according to ASTM C1314-14 [17] were also included in the test groups. The number of experiments was kept large enough to provide statistical data. The correlation between prism and infill wall strength was established with a valid and practical method in terms of expected, lower-bound, and upper-bound approach. Consistency between the experimental and analytical results were also discussed. In this section, the significant outcomes of the study were summarized. In addition, recommendations were also made based on the experience gained in this research.

Diagonally loaded and plastered single brick prism group, SDP-1, successfully and sufficiently estimated the experimental infill wall strength for expected, upper-bound, and lower bound strengths by the adopted equation based on ASCE/SEI 41-17 [15]. In other words, results were almost equal to the experimental infill wall strengths. Diagonal testing of prism is highly encouraged via the apparatus similar to one used in this study.

Table 4 Comparison of analytical infill wall strengths due to prism tests

Specimen group	f'_{me} (MPa)	STD (MPa)	V_{infe} (kN)	V_{infl} (kN)	V_{infu} (kN)	Ratio of analytical to experimental strength		
						V_{infe}	V_{infl}	V_{infu}
SVB-2	3.94	0.36	121.0	109.9	132.0	1.3	1.40	1.28
SHB-2	1.07	0.18	32.9	27.3	38.4	0.4	0.35	0.37
SVP-2	4.30	0.28	132.0	123.4	140.6	1.5	1.57	1.36
SHP-2	1.88	0.27	57.7	49.4	66.0	0.6	0.63	0.64
SVP-1	4.16	1.21	127.7	90.6	164.9	1.4	1.16	1.60
SHP-1	1.92	0.54	59.0	42.4	75.5	0.6	0.54	0.73
SDP-1	2.96	0.46	90.9	76.8	105.0	1.0	0.98	1.02
SVB-1	4.04	0.95	124.1	94.9	153.2	1.4	1.21	1.48
SHB-1	1.18	0.47	36.2	21.8	50.7	0.4	0.28	0.49
SDB-1	2.51	0.76	77.1	53.7	100.4	0.8	0.69	0.97

While vertically loaded prism group constantly over-estimated the experimental infill wall strengths, horizontally loaded prism group constantly under-estimated those strength values. Both cases were considered beyond acceptable limits. It should be emphasized that results also included the tests and prisms according to ASTM C1314-14 [17]. On the other hand, if diagonal testing is not possible to conduct, the average of the vertically and horizontally loaded prism tests may be used instead.

Presence of a plaster on the prism had considerable impact on determining infill wall lateral load capacity. Thus, prisms should be covered with a plaster as in the actual condition of infill walls. Additionally, load capacity of the bare brick plus halve load capacity of the plaster gave accurate results for calculating the load capacity of the plastered prism. In other words, if only the strength of bare prisms is available, 50% of the plaster equivalent cylinder strength multiplied by its cross-sectional area may be included in the calculations to obtain the load capacity of the plastered prism.

Prisms composed of double bricks and formed according to ASTM C1314-14 [17] had strengths consistent with the corresponding prisms composed of a single brick if correction factors for the aspect ratios are used. As known,

ASTM C1314-14 [17] requires building prisms with minimum two bricks with mortar beds. As a result, heights of prism specimens are generally too large for compression machines which are originally produced for concrete cylinder specimens. Instead of that labor-intensive and time-consuming process, single brick prisms may be successfully used due to practical reasons.

While FEMA-306 [12] focusses on expected strength of infill walls, ASCE/SEI 41-17 [15] focusses on lower-bound strength for a safer approach. Eventual high standard deviations for infill walls in terms of strength, forces the designers to use lower-bound strength due to the concerns of safety. However, it is not always safer to use the lower-bound strength. For example, if the designer should check the shear resistance of the surrounding RC frame owing to the loads acting from the infill wall, it would be appropriate to use the upper-bound instead of the lower-bound. On the other hand, it is safer to use lower-bound strength to include the stiffness and strength contribution of infill walls to the structural system. As a result, the use of lower-bound should be encouraged when the expected strength is in favor and the use of upper-bound should be encouraged when the expected strength is considered disadvantageous.

References

- [1] Haris, I., Hortobágyi, Z. "Different FEM models of reinforced concrete frames stiffened by infill masonry for lateral loads", *Periodica Polytechnica Civil Engineering*, 56(1), pp. 25–34, 2012. <https://doi.org/10.3311/pp.ci.2012-1.03>
- [2] Haldar, P., Singh, Y., Paul, D. K. "Identification of seismic failure modes of URM infilled RC frame buildings", *Engineering Failure Analysis*, 33, pp. 97–118, 2013. <https://doi.org/10.1016/j.engfailanal.2013.04.017>
- [3] Cavaleri, L., Di Trapani, F. "Prediction of the additional shear action on frame members due to infills", *Bulletin of Earthquake Engineering*, 13, pp. 1425–1454, 2015. <https://doi.org/10.1007/s10518-014-9668-z>
- [4] Moretti, M. L. "Seismic design of masonry and reinforced concrete infilled frames: a comprehensive overview", *American Journal of Engineering and Applied Sciences*, 8(4), pp. 748–766, 2015. <https://doi.org/10.3844/ajeassp.2015.748.766>
- [5] Di Trapani, F., Macaluso, G., Cavaleri, L., Papia, M. "Masonry infills and RC frames interaction: literature overview and state of the art of macromodeling approach", *European Journal of Environmental and Civil Engineering*, 19(9), pp. 1059–1095, 2015. <https://doi.org/10.1080/19648189.2014.996671>
- [6] Basha, S. H., Kaushik, H. B. "Predicting shear failure in columns of masonry infilled rc frames using macro-modeling approach", In: *16th World Conference on Earthquake Engineering*, 16WCEE 2017, Santiago, Chile, 2017, Paper No. 3168.
- [7] Özbek, E., Aykaç, B., Can, H., Kalkan, İ., Aykaç, S. "Recommendations for calculation of strengthened brick walls with perforated plates", *Journal of the Faculty of Engineering and Architecture of Gazi University*, 34(1), pp. 1–15, 2019. [online] Available at: <https://dergipark.org.tr/tr/download/article-file/677180> (In Turkish)
- [8] Haris, I., Farkas, G. "Experimental Results on Masonry Infilled RC Frames for Monotonic Increasing and Cyclic Lateral Load", *Periodica Polytechnica Civil Engineering*, 62(3), pp. 772–782, 2018. <https://doi.org/10.3311/PPci.10715>
- [9] Mohammadi, M., Nikfar, F. "Strength and Stiffness of Masonry-Infilled Frames with Central Openings Based on Experimental Results", *ASCE Journal of Structural Engineering*, 139(6), pp. 974–984, 2013. [https://doi.org/10.1061/\(ASCE\)ST.1943-541X.0000717](https://doi.org/10.1061/(ASCE)ST.1943-541X.0000717)
- [10] Kakaletsis, D. J., Karayannis, C. G. "Influence of Masonry Strength and Openings on Infilled R/C Frames Under Cycling Loading", *Journal of Earthquake Engineering*, 12(2), pp. 197–221, 2008. <https://doi.org/10.1080/13632460701299138>
- [11] Mansouri, A., Marefat, M. S., Khanmohammadi, M. "Analytical estimation of lateral resistance of low-shear strength masonry infilled reinforced concrete frames with openings", *Structural Design of Tall and Special Buildings*, 27(6), e1452, 2018. <https://doi.org/10.1002/tal.1452>
- [12] Applied Technology Council (ATC-43 Project) "FEMA 306 Evaluation of Earthquake Damaged Concrete and Masonry Wall Buildings", Federal Emergency Management Agency, Washington DC, USA, 1998.

- [13] Haris, I., Hortobágyi, Z. "Comparison of Experimental and Analytical Results on Masonry Infilled RC Frames for Cyclic Lateral Load", *Periodica Polytechnica Civil Engineering*, 59(2), pp. 193–208, 2015.
<https://doi.org/10.3311/PPci.8099>
- [14] Haris, I., Hortobágyi, Z. "Comparison of experimental and analytical results on masonry infilled RC frames for monotonic increasing lateral load", *Periodica Polytechnica Civil Engineering*, 56(2), pp. 185–196, 2012.
<https://doi.org/10.3311/pp.ci.2012-2.05>
- [15] ASCE "ASCE/SEI 41-17 Seismic Evaluation and Retrofit of Existing Buildings", American Society of Civil Engineers, Reston, VI, USA, 2017.
<https://doi.org/10.1061/9780784414859>
- [16] Masonry Standards Joint Committee (MSJC) "TMS 402/602-13 Building Code Requirements and Specification for Masonry Structures", The Masonry Society, Longmont, CO, USA, 2013.
- [17] ASTM "ASTM C1314-14 Standard Test Method for Compressive Strength of Masonry Prisms", American Society for Testing and Materials, West Conshohocken, PA, USA, 2014.
<https://doi.org/10.1520/C1314-14>
- [18] Wells, J. C. "History of structural hollow clay tile in the United States", *Construction History*, 22, pp. 27–46, 2007.
- [19] Ferreira, D., Caldeirinha, R. F. S., Fernandes, T. R., Cuiñas, I. "Hollow clay brick wall propagation analysis and modified brick design for enhanced wi-fi coverage", *IEEE Transactions on Antennas and Propagation*, 66(1), pp. 331–339, 2018.
<https://doi.org/10.1109/TAP.2017.2772028>
- [20] Antoniadis, K. D., Assael, M. J., Tsiglifisi, C. A., Mylona, S. K. "Improving the design of Greek hollow clay", *International Journal of Thermophysics*, 33, pp. 2274–2290, 2012.
<https://doi.org/10.1007/s10765-012-1294-x>
- [21] Cavaco, E., Grilo, I., Gouveia, J. P., Júlio, E., Neves, L. "Mechanical performance of eco-efficient hollow clay bricks incorporating industrial nano-crystalline aluminium sludge", *European Journal of Environmental and Civil Engineering*, 24(12), pp. 1921–1938, 2018.
<https://doi.org/10.1080/19648189.2018.1492974>
- [22] Özbek, E., Aykaç, B., Aykaç, S. "The effects of brick walls strengthened with perforated steel plates on frame behavior", *Engineering Structures*, 189, pp. 62–76, 2019.
<https://doi.org/10.1016/j.engstruct.2019.03.080>
- [23] Baran, M., Aktaş, M., Aykaç, S. "Strengthening of plastered hollow brick infill walls using strip concrete/reinforced concrete panels", *Journal of the Faculty of Engineering and Architecture of Gazi University*, 29(1), pp. 23–33, 2014. (In Turkish)
<https://doi.org/10.17341/gummfd.43725>
- [24] Azevedo, A., Delgado, J.Q., Guimaraes, A., Silva, F. A., Oliveira, R. "Compression behaviour of clay bricks prisms, wallets and walls-Coating influence", *Revista de la Construcción*, 18(1), pp. 123–133, 2019.
<https://doi.org/10.7764/rdlc.18.1.123>
- [25] Arslan, M. E., Agcakoca, E., Şentürk, M. "The Effects of Plaster Thicknesses on Cyclic Behavior of Infill Walls with Different Materials", *Periodica Polytechnica Civil Engineering*, 64(3), pp. 678–689, 2020.
<https://doi.org/10.3311/PPci.15555>
- [26] Fódi, A. "Effects influencing the compressive strength of a solid, fired clay brick", *Periodica Polytechnica Civil Engineering*, 55(2), pp. 117–128, 2011.
<https://doi.org/10.3311/pp.ci.2011-2.04>
- [27] TSI "TS EN 771-1 Specification for masonry units -Part 1: Clay masonry units", Turkish Standards Institution, Ankara, Turkey, 2005.
- [28] International Working Group on Reinforced Concrete "Reinforced Concrete: An International Manual", UNESCO, 1971. ISBN 0 408 70175 7
- [29] ASTM "ASTM C109 Standard Test Method for Compressive Strength of Hydraulic Cement Mortars (Using 2-in or [50-mm] Cube Specimens)", American Society for Testing and Materials, West Conshohocken, PA, USA, 2021.
https://doi.org/10.1520/C0109_C0109M-21
- [30] TSI "TS 12390-3 Testing hardened concrete compressive strength of test specimens", Turkish Standards Institution, Ankara, Turkey, 2019.